JCB Article

Loss of proteolytically processed filaggrin caused by epidermal deletion of Matriptase/MT-SP1

Karin List,[1,6] Roman Szabo,[1] Philip W. Wertz,[3] Julie Segre,[2] Christian C. Haudenschild,[4] Soo-Youl Kim,[5] and Thomas H. Bugge[1]

[1]Proteases and Tissue Remodeling Unit, National Institute of Dental and Craniofacial Research, and [2]National Human Genome Research Institute, National Institutes of Health, Bethesda, MD 20892
[3]Dows Institute, University of Iowa College of Dentistry, Iowa City, IA 52242
[4]Department of Experimental Pathology, American Red Cross, Rockville, MD 20855
[5]Department of Neuroscience, Weill Medical College of Cornell University and Burke Medical Research Institute, White Plains, NY 10605
[6]Finsen Laboratory, DK-2100 Copenhagen, Denmark

Profilaggrin is a large epidermal polyprotein that is proteolytically processed during keratinocyte differentiation to release multiple filaggrin monomer units as well as a calcium-binding regulatory NH_2-terminal filaggrin S-100 protein. We show that epidermal deficiency of the transmembrane serine protease Matriptase/MT-SP1 perturbs lipid matrix formation, cornified envelope morphogenesis, and stratum corneum desquamation. Surprisingly, proteomic analysis of Matriptase/MT-SP1–deficient epidermis revealed the selective loss of both proteolytically processed filaggrin monomer units and the NH_2-terminal filaggrin S-100 regulatory protein. This was associated with a profound accumulation of profilaggrin and aberrant profilaggrin-processing products in the stratum corneum. The data identify keratinocyte Matriptase/MT-SP1 as an essential component of the profilaggrin-processing pathway and a key regulator of terminal epidermal differentiation.

Introduction

The epidermis provides a permeability barrier that prevents excessive water loss to the surrounding environment. To perform this function, epidermal keratinocytes arise from proliferating basal cells and move outward through a series of distinct differentiation events to form the stratum corneum, a two-compartment structure that consists of a lipid-enriched ECM in which an interlocking meshwork of dead corneocytes are embedded (Roop, 1995; Nemes and Steinert, 1999; Presland and Dale, 2000). Epidermal differentiation culminates with the regulated shedding (desquamation) of the outermost layer of corneocytes to control the thickness of the stratum corneum (Egelrud, 2000; Pierard et al., 2000). Water impermeability is conferred by the intercorneocyte lipid matrix, and by an insoluble cornified envelope (CE) that is deposited on the inner surface of the plasma membrane of the corneocytes. The intercorneocyte lipid matrix consists of a complex lipid mixture that self-assembles into an ordered multilayer structure known as lipid lamellae (Landmann, 1986; Elias and Menon, 1991; Wertz, 2000). These lipids are synthesized during the final stages of epidermal differentiation by ubiquitously expressed and epidermis-specific lipid biogenesis enzymes (Elias and Menon, 1991; Wertz and van den Bergh, 1998).

The CE is assembled from an array of epidermis-specific proteins that are coordinately expressed during late stages of epidermal differentiation, and are linked together by N^{ε}-(γ-glutamyl)-lysine isopeptide bonds. Furthermore, a monomolecular layer of ceramides is covalently attached to the outer surface of the CE to form a hydrophobic lipid envelope that covers each corneocyte and provides continuity with the lipid matrix (Swartzendruber et al., 1987; Wertz et al., 1989; Marekov and Steinert, 1998).

Profilaggrin is a major epidermal proprotein that undergoes extensive proteolytic modification during terminal differentiation. It is synthesized as a large (>300 kD), extremely insoluble phosphoprotein that consists of a unique

K. List and R. Szabo contributed equally to this paper.

Address correspondence to Thomas H. Bugge, Proteases and Tissue Remodeling Unit, Oral and Pharyngeal Cancer Branch, National Institute of Dental and Craniofacial Research, National Institutes of Health, 30 Convent Drive, Room 211, Bethesda, MD 20892. Tel.: (301) 435-1840. Fax: (301) 402-0823. email: thomas.bugge@nih.gov

Key words: barrier function; lipid lamellar bodies; membrane serine protease; profilaggrin; stratum corneum

Abbreviations used in this paper: CE, cornified envelope; E, embryonic day.

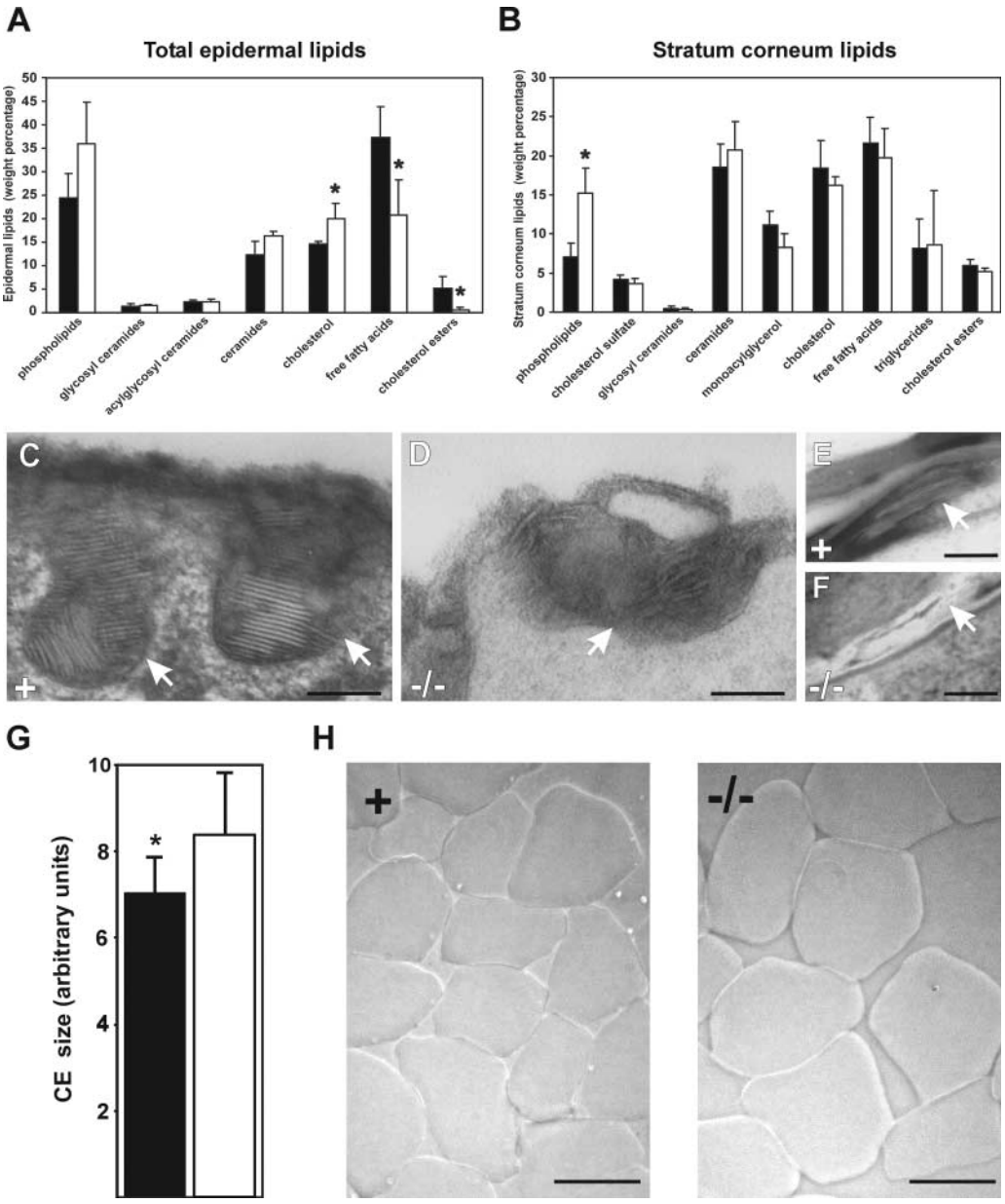

Figure 1. **Matriptase/MT-SP1–deficient mice are born with epidermal lipid matrix defects and enlarged CEs.** Total epidermal (A) and stratum corneum (B) lipids in Matriptase/MT-SP1$^{-/-}$ (open bars, $n = 3$) and control (solid bars, $n = 3$) neonates (mean weight percentage of total lipids ± SD). (A) *, $P < 0.04$ and (B) *, $P < 0.02$ (two-tailed t test). (C–F) Ultrastructural appearance of transitional cells (C and D) and stratum corneum (E and F) of control epidermis (C and E) and Matriptase/MT-SP1$^{-/-}$ epidermis (D and F) of ruthenium-stained sections. (C) Lipid lamellar bodies with well-aligned lipid stacks (arrows) at the interface between the transitional layer and stratum corneum in control epidermis. (D) Rare and poorly formed lamellar bodies (arrow) with wavy, short, and disorganized lipid structures in Matriptase/MT-SP1$^{-/-}$ epidermis. (E) Highly ordered intercorneocyte lipid lamellar membranes (arrow) in control stratum corneum. (F) Poorly formed intercorneocyte lipid lamellae in Matriptase/MT-SP1$^{-/-}$ stratum corneum (arrow). (G) Average surface area of newborn Matriptase/MT-SP1$^{-/-}$ (open bar, $n = 70$) and littermate control (solid bar; $n = 50$) CEs (mean ± SD; *, $P < 0.004$; two-tailed t test). The experiment was repeated three times with similar results. (H) Morphological appearance of purified CEs from Matriptase/MT-SP1$^{-/-}$ epidermis (right panel) and littermate control epidermis (left panel) visualized by phase-contrast light microscopy. Bars: (C–F) 100 nm, (H) 30 μm.

NH_2-terminal Ca^{2+}-binding protein of the S-100 family, linked to 10–20 tandem filaggrin monomer repeats (Rothnagel and Steinert, 1990; Presland et al., 1992; Zhang et al., 2002). During terminal epidermal differentiation, the linker regions connecting the NH_2-terminal S-100 protein and each individual filaggrin repeat are completely removed by proteolysis to generate two major products: mature filaggrin monomer and the NH_2-terminal S-100 protein (Resing et al., 1984; Presland et al., 1997). Four different functions have been described for these profilaggrin-processing products: (1) the filaggrin monomer aids keratin aggregation during the formation of macrofibril bundles (Dale et al., 1978); (2) filaggrin monomers are a component of the CE, and may constitute as much as 10% of total cross-linked CE protein (Steven and Steinert, 1994); (3) filaggrin monomer is completely degraded in the uppermost layers of the stratum corneum to produce a mixture of free modified hygroscopic amino acids that are important for maintaining

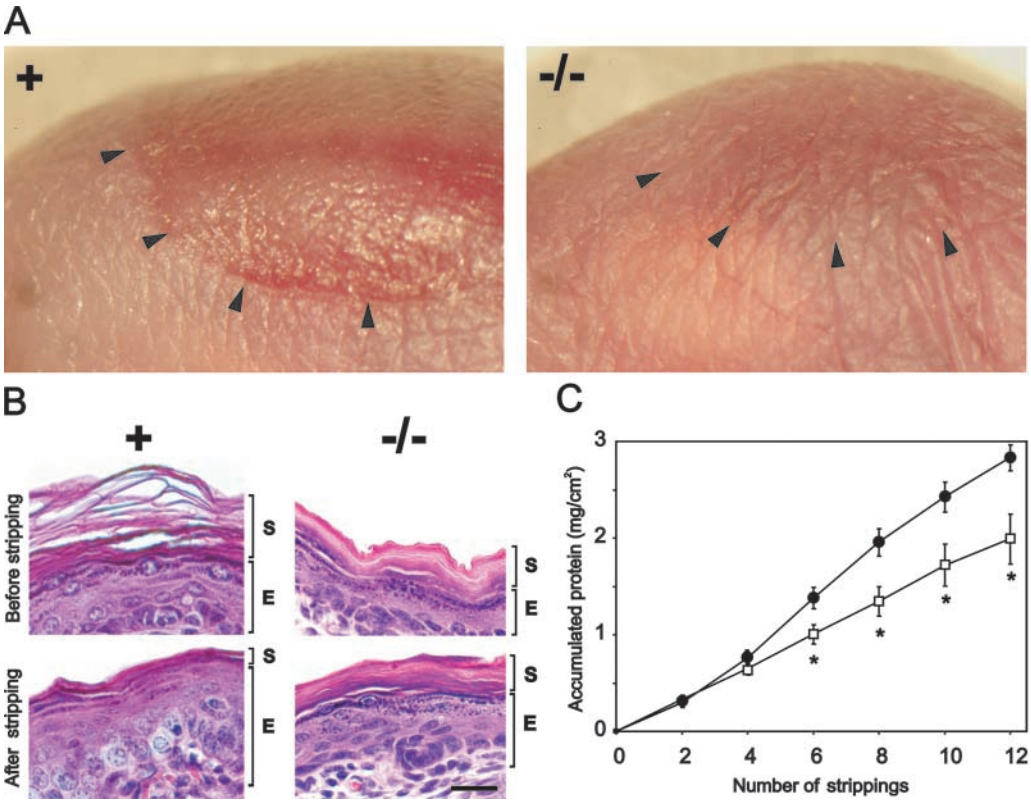

Figure 2. **Impaired desquamation of newborn Matriptase/MT-SP1–deficient stratum corneum.** (A) Macroscopic appearance of neonatal dorsal skin of control (left) and littermate Matriptase/MT-SP1$^{-/-}$ (right) after 12 sequential applications of adhesive-coated discs. The stratum corneum is completely removed from the tape-stripped area of the control epidermis, exposing the lower epidermal layers, whereas only minimal defects are apparent in Matriptase/MT-SP1$^{-/-}$ epidermis subjected to the same treatment. Arrowheads indicate the outline of the tape-stripped area. (B) Microscopic appearance of control (left panels) and littermate Matriptase/MT-SP1$^{-/-}$ (right panels) epidermis before (top panels) and after (bottom panels) 12 rounds of tape stripping. Complete removal of the stratum corneum with exposed upper granular and transitional cell layers in control mice and minimal stratum corneum removal in Matriptase/MT-SP1$^{-/-}$ epidermis. Hematoxylin and eosin staining. "E" indicates the location of basal and suprabasal epidermis, and "S" indicates the location of the stratum corneum. Bars, 20 μm. (C) Accumulated removal of extractable stratum corneum proteins from Matriptase/MT-SP1$^{-/-}$ (open squares, $n = 7$) and littermate control (closed circles, $n = 7$) mice after tape stripping (± SEM; *, $P < 0.03$; two-tailed t test).

epidermal hydration (Scott and Harding, 1986; Rawlings et al., 1994); and (4) the NH_2-terminal filaggrin S-100 protein translocates to the nucleus after being proteolytically liberated, and is believed to function as a calcium-dependent transcriptional regulator of genes that are associated with late stratum corneum differentiation (Pearton et al., 2002; Zhang et al., 2002).

Two factors have greatly complicated the analysis of profilaggrin processing. First, expression of recombinant profilaggrin is problematic due to its large size and extreme insolubility. Second, the processing of profilaggrin is difficult to mimic in cultured keratinocytes because only incomplete processing can be observed after calcium-induced differentiation (Pearton et al., 2002). However, several proteases, believed to partake in profilaggrin processing, have been described. These include members of the proprotein convertase family (e.g., furin), calpain-1, and a serine protease of unknown identity termed profilaggrin endopeptidase 1 (PEP1; Resing et al., 1993, 1995; Pearton et al., 2001). Furin has been proposed to cleave the NH_2 terminus of profilaggrin, facilitating the release of the NH_2-terminal S-100 protein (Pearton et al., 2001). In contrast, calpain-1 and PEP1 are both implicated in the processing of the linker regions between the filaggrin monomer repeats to generate the free filaggrin monomer (Resing et al., 1993, 1995; Pearton et al., 2001).

Matriptase/MT-SP1 is a novel type II transmembrane serine protease that is expressed by most cells of epithelial origin, including keratinocytes (Kim et al., 1999; Lin et al., 1999; Takeuchi et al., 1999; Oberst et al., 2001). Recently, we demonstrated that a targeted deletion of Matriptase/MT-SP1 leads to the loss of epidermal barrier function in newborn mice (List et al., 2002). We now show that keratinocyte-expressed Matriptase/MT-SP1 regulates three key steps in stratum corneum function—lipid matrix formation, CE morphogenesis, and desquamation—and we link the pleiotropic effects of epidermal loss of Matriptase/MT-SP1 to defective proteolytic processing of profilaggrin.

Results

Matriptase/MT-SP1–deficient mice are born with epidermal lipid matrix defects, abnormal CEs, and impaired desquamation

To understand the barrier function defect caused by Matriptase/MT-SP1 deficiency, lipid matrix, CE formation, and desquamation were analyzed in neonates (Fig. 1 and

Fig. 2). Interestingly, several distinct changes were detected in total epidermal (Fig. 1 A) and stratum corneum (Fig. 1 B) lipids of Matriptase/MT-SP1$^{-/-}$ neonates. Free fatty acids were decreased almost 50% in Matriptase/MT-SP1$^{-/-}$ epidermis, whereas cholesterol was increased by ~25%, and its derivatives, sterol esters, displayed an almost 10-fold decrease (Fig. 1 A). Furthermore, the phospholipid content was more than doubled in Matriptase/MT-SP1$^{-/-}$ stratum corneum, rendering phospholipids a major intercorneocyte lipid component; other lipids were present in similar proportions to control mice (Fig. 1 B). Ultrastructural analysis of ruthenium tetroxide–preserved epidermal lipid structures showed that the abnormal epidermal lipid composition seriously compromised lipid matrix assembly. Compared with control mice, lamellar bodies were extremely sparse in the granular layer of neonatal Matriptase/MT-SP1$^{-/-}$ epidermis and presented as wavy, short, and disorganized lipid structures (Fig. 1, C and D). Likewise, the intercorneocyte lipids were poorly organized with short and misaligned lipid lamellae (Fig. 1, E and F). These data demonstrate that Matriptase/MT-SP1 is essential for stratum corneum lipid matrix formation.

CEs were isolated from Matriptase/MT-SP1$^{-/-}$ neonates to assess their morphology and mechanical integrity. Interestingly, the Matriptase/MT-SP1$^{-/-}$ CEs were 15% larger than the CEs isolated in parallel from littermate controls, revealing a distinct alteration in CE morphogenesis (Fig. 1 G). However, Matriptase/MT-SP1$^{-/-}$ CEs displayed no alterations in shape or surface appearance when examined by light microscopy (Fig. 1 H) or scanning EM (unpublished data), or a decreased mechanical strength, as measured by the resistance to ultrasound treatment (unpublished data). In accordance with the latter observations, the expression level and the enzymatic activity of transglutaminase-1, -2, and -3 were unaffected by the loss of Matriptase/MT-SP1 (unpublished data).

Next, we subjected newborn Matriptase/MT-SP1$^{-/-}$ epidermis to a tape-stripping procedure routinely used to assess stratum corneum integrity (Marttin et al., 1996; Dreher et al., 1998). Adhesive-coated discs were repeatedly applied to the dorsal skin, and stratum corneum removal was analyzed by visual inspection, histological analysis, and quantitation of stratum corneum protein loss. The entire stratum corneum of control mice was lost after 12 successive rounds of tape stripping, leaving the lower layers of the epidermis exposed (Fig. 2, A and B; left panels). However, the same procedure barely affected the Matriptase/MT-SP1$^{-/-}$ stratum corneum (Fig. 2, A and B; right panels). This increased mechanical resistance of Matriptase/MT-SP1$^{-/-}$ epidermis was further evidenced by a significant reduction in stratum corneum protein loss after tape stripping, as determined by the quantitation of total protein adhering to adhesive-coated discs applied to Matriptase/MT-SP1 and control skin (Fig. 2 C).

Loss of mature filaggrin monomer in neonate Matriptase/MT-SP1–deficient epidermis

Analysis of newborn Matriptase/MT-SP1$^{-/-}$ epidermis by cDNA array hybridization, Western blot analysis, immunohistochemistry, or two-dimensional gel electrophoresis did not unravel significant changes in the expression of epidermal differentiation–associated structural genes (Fig. 3 B; unpublished data). Surprisingly, however, Matriptase/MT-SP1$^{-/-}$ epidermal protein extracts separated by SDS-PAGE lacked a major protein of ~32 kD (Fig. 3 A, lanes 1 and 2). The 32-kD protein was not expressed in detectable amounts in the dermis (Fig. 3 A, lanes 3 and 4) or in a number of tissues that developed normally in Matriptase/MT-SP1$^{-/-}$ mice (unpublished data), suggesting that the absence of this protein could be causally related to the epidermal phenotype in the mutant mice. To identify the 32-kD protein product, extracts from Matriptase/MT-SP1$^{-/-}$ and littermate control epidermis were separated by preparative SDS-PAGE. Proteins within the 32-kD size range were then subjected to in-gel tryptic digestion, followed by differential mass spectrometry–based peptide mapping. This analysis identified six peptides that were exclusively present in the control epidermis. All six peptides could unambiguously be assigned as being derived from mouse filaggrin (Table I). This result was confirmed by the absence of immunoreactive material within the 32-kD range in Western blot analysis of extracts of Matriptase/MT-SP1$^{-/-}$

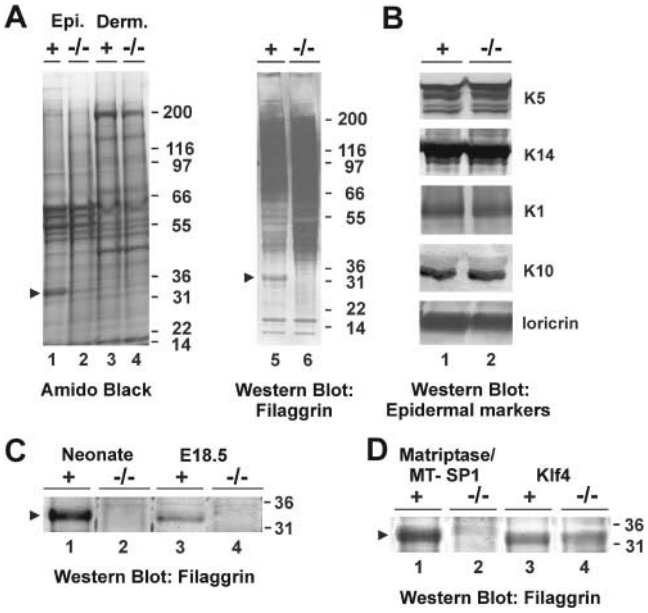

Figure 3. **Matriptase/MT-SP1–deficient epidermis lacks proteolytically processed filaggrin monomer.** (A) Amido black staining (lanes 1–4) of SDS-PAGE–separated protein extracts from epidermis (lanes 1 and 2) and dermis (lanes 3 and 4), and whole-skin extract filaggrin monomer Western blot (lanes 5 and 6) of control (lanes 1, 3, and 5) and littermate Matriptase/MT-SP1$^{-/-}$ (lanes 2, 4, and 6) neonates. (B) Western blot analysis of SDS-PAGE–separated proteins from skin from control (lane 1) and littermate Matriptase/MT-SP1$^{-/-}$ (lane 2) neonates using antibodies against the basal layer markers keratin-5 and -14, the suprabasal layer markers keratin-1 and -10, and the granular layer/stratum corneum marker loricrin. (C) Western blot analysis of total skin protein extracts from neonates (lanes 1 and 2) and E18.5 embryos (lanes 3 and 4) from control (lanes 1 and 3) and littermate Matriptase/MT-SP1$^{-/-}$ (lanes 2 and 4) mice using the filaggrin monomer repeat antibody. (D) Western blot of total skin protein extracts from newborn control (lane 1), littermate Matriptase/MT-SP1$^{-/-}$ (lane 2), Klf4 control (lane 3), and littermate Klf4$^{-/-}$ (lane 4) neonates using the filaggrin monomer repeat antibody. Arrowheads in A, C, and D indicate the 32-kD filaggrin monomer immunoreactive protein specifically missing in Matriptase/MT-SP1$^{-/-}$ epidermis. The positions of mol wt markers (kD) are indicated.

Table I. **Identification of filaggrin as the protein absent in Matriptase/MT-SP1–deficient skin by mass spectrometry**

Measured mass	Theoretical mass[a]	Residue no.	Sequence
D	*D*		
2461.4	2461.5	117–136	(R)GHQHQHQHQHEHEQPESGHR(Q)
2197.1	2197.3	206–226	(R)QPSPSQSSDSQVHSGVQVEGR (R)
2354.3	2353.5	206–227	(R)QPSPSQSSDSQVHSGVQVEGRR (G)
2721.9	2721.5	202–226	(R)DRPRQPSPSQSSDSQVHSGVQVEGR (R)
2632.6	2632.6	45–70	(R)GVSESQASDSEGHSDFSEGQAVGAHR (Q)
2788.2	2788.8	44–70	(R)RGVSESQASDSEGHSDFSEGQAVGAHR(Q)

Skin lysates from newborn Matriptase/MT-SP1$^{-/-}$ mice and littermate controls were separated by SDS-PAGE, and proteins were stained with amido black. Two corresponding gel pieces, in the region where a major protein appeared to be absent in the Matriptase/MT-SP1$^{-/-}$ mice, were excised from parallel lanes containing skin lysates from Matriptase/MT-SP1$^{-/-}$ mice and control mice, and were subjected to in-gel trypsin digestion. The fragments listed represent peptides that were prominent in the control skin and were nondetectable in the Matriptase/MT-SP1$^{-/-}$ skin.
[a]Theoretical average masses were derived from the National Center for Biotechnology Information database identifying mouse filaggrin B (GenBank/EMBL/DDBJ accession no. B35026).

skin using a filaggrin monomer repeat antibody (Fig. 3 A, lanes 5 and 6). Together, the data show that epidermal Matriptase/MT-SP1 deletion correlates with the loss of detectable filaggrin monomer in the absence of overt changes in the expression of other abundant epidermal proteins.

Loss of filaggrin monomer is not secondary to the loss of epidermal barrier function

Two separate strategies were used to determine whether the loss of filaggrin monomer in Matriptase/MT-SP1$^{-/-}$ epidermis was caused by a compensatory increase in filaggrin turnover secondary to the loss of epidermal barrier function (Scott and Harding, 1986; Rawlings et al., 1994), or if it was the direct consequence of the loss of Matriptase/MT-SP1. First, filaggrin expression was analyzed in the epidermis from embryonic day 18.5 (E18.5) embryos immediately after delivery by Caesarian section. This procedure excluded potential effects on filaggrin turnover caused by postpartum air exposure and dehydration. The 32-kD filaggrin monomer was readily detected in E18.5 control epidermis by Western blot analysis using a filaggrin monomer repeat antibody (Fig. 3 C, lane 3), but was present in substantially lower amounts than in neonate control skin (Fig. 3 C, lane 1), as reported previously (Hardman et al., 1998). In contrast, no filaggrin protein was detected in E18.5 Matriptase/MT-SP1$^{-/-}$ epidermis (Fig. 3 C, lane 4), demonstrating that the loss of filaggrin monomer occurs before birth and exposure to a dehydrating terrestrial environment. Second, the expression of filaggrin in neonatal epidermis from Klf4$^{-/-}$ mice was analyzed. These mutant mice display a complete loss of skin barrier function leading to perinatal death due to dehydration, and they phenotypically closely resemble Matriptase/MT-SP1$^{-/-}$ mice (Segre et al., 1999). However, Western blot analysis showed normal expression of filaggrin monomer in the epidermis of newborn Klf4$^{-/-}$ pups (Fig. 3 D, compare lane 3 with lane 4). Together, the data show that the loss of filaggrin monomer is not secondary to the loss of barrier function and epidermal dehydration.

Proteolytic processing of profilaggrin is defective in Matriptase/MT-SP1–deficient epidermis

Profilaggrin accumulates in large quantities in the granular layer of the epidermis, where it undergoes extensive post-translational processing by endoproteolytic cleavage in the transitional cell layer to produce the mature filaggrin monomer. To analyze the function of Matriptase/MT-SP1 in profilaggrin processing, the epidermis from pairs of newborn Matriptase/MT-SP1$^{-/-}$ and control pups were subjected to NaSCN extraction, precipitation, and urea solubilization of extracted proteins. This extraction procedure results in the purification of profilaggrin and its proteolytic products to >90% homogeneity (Resing et al., 1984), and permitted a detailed analysis of profilaggrin processing. Protein extracts from normal epidermis prepared this way contain predominantly the 32-kD filaggrin monomer, quantitatively minor amounts of higher mol wt complexes of filaggrin-processing intermediates, and profilaggrin, which appear as a regularly spaced "ladder" of proteins after separation by SDS-PAGE (Fig. 4 A, lanes 1 and 3; Resing et al., 1984). In striking contrast, the 32-kD filaggrin monomer could not be detected in extracts prepared from Matriptase/MT-SP1$^{-/-}$ epidermis, confirming the requirement of the serine protease for filaggrin monomer generation (Fig. 4 A, lanes 2 and 4). Instead, these extracts contained highly increased amounts of profilaggrin and aberrant filaggrin processing intermediates. The pronounced accumulation of profilaggrin and the aberrant profilaggrin-processing products in Matriptase/MT-SP1$^{-/-}$ epidermis were not associated with a detectable increase in profilaggrin mRNA, as determined by both Northern blot analysis and cDNA array hybridization (unpublished data).

Aberrantly processed profilaggrin products incorporate in corneocytes during terminal differentiation of Matriptase/MT-SP1–deficient epidermis

Profilaggrin is sequestered in cytoplasmic nonmembrane-bound insoluble keratohyalin filaggrin granules (F-granules) in the granular layer, is proteolytically processed and released from F-granules during terminal differentiation, and is incorporated into the CEs of corneocytes (Steinert and Marekov, 1995; Simon et al., 1996). Immuno-EM of Matriptase/MT-SP1$^{-/-}$ epidermis was used to determine the ultrastructural location and fate of profilaggrin in the absence of normal processing. Examination of the F-granules in the granular layer did not reveal significant changes in the staining intensity between Matriptase/MT-SP1–deficient and –sufficient epidermis (Fig. 4, B and C), compatible with the normal microscopic and ultrastructural appearance of F-granules (List et al., 2002). In terminally differentiated

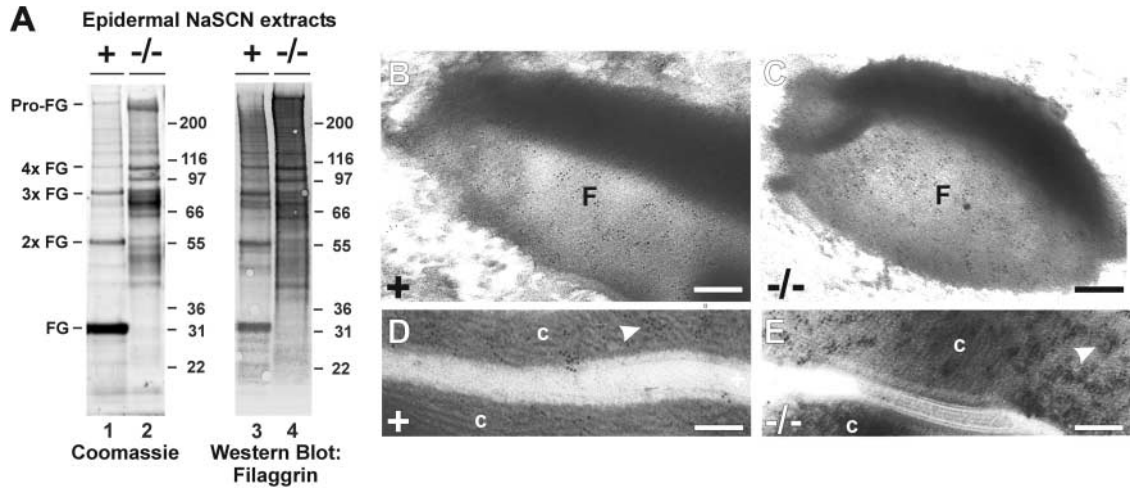

Figure 4. **Defective proteolytic processing of profilaggrin and incorporation of aberrantly processed profilaggrin into the stratum corneum of Matriptase/MT-SP1–deficient epidermis.** (A) Profilaggrin (Pro-FG) and profilaggrin-derived (FG) proteins were partially purified by NaSCN and urea extraction of the skin of control (lanes 1 and 3) and littermate Matriptase/MT-SP1$^{-/-}$ (lanes 2 and 4) neonates. 50 (lanes 1 and 2) or 0.5 (lanes 3 and 4) μg protein was separated by SDS-PAGE under reducing conditions and stained with Coomassie brilliant blue (lanes 1 and 2) or subjected to Western blot analysis with a filaggrin monomer antibody (lanes 3 and 4). The positions of profilaggrin-related protein products are indicated on the left, and the positions of mol wt markers (kD) on the right. (B–E) Representative examples of filaggrin immuno-EM of filaggrin granules (F) in granular layer cells (B and C), and corneocytes ("c" in D and E) from littermate control (B and D) and Matriptase/MT-SP1$^{-/-}$ (C and E) epidermis. Filaggrin antibody binding was visualized with colloidal gold-labeled secondary antibodies. Both filaggrin granules in granular layer cells (B and C) and keratin aggregates of terminally differentiated corneocytes (D and E, arrowheads) display intense gold labeling, indicative of incorporation of profilaggrin immunoreactive material, with no detectable differences in the labeling intensity in control and Matriptase/MT-SP1$^{-/-}$ epidermis. Bars: (B and C) 100 nm, (D and E) 75 nm.

corneocytes, filaggrin-immunoreactive material was profuse in the central and peripheral keratin aggregates in both Matriptase/MT-SP1$^{-/-}$ and control epidermis (Fig. 4, D and E). In conclusion, the data suggest that unprocessed or aberrantly processed profilaggrin is released from F-granules and incorporates into terminally differentiated corneocytes.

Matriptase/MT-SP1 deficiency impairs proteolytic liberation of profilaggrin S-100 protein

The sequential proteolytic liberation of the NH_2-terminal filaggrin S-100 protein is required for its nuclear translocation during terminal epidermal differentiation (Pearton et al., 2002). Western blot analysis of epidermal extracts from control mice using a peptide antibody directed against the NH_2-terminal A domain of the profilaggrin S-100 protein revealed the mature S-100 protein as well as several processing intermediates that have been characterized previously (Fig. 5, lane 1). These included doublet proteins of 28–30 kD, corresponding to the intact, proteolytically liberated S-100 protein, and a 16-kD protein, corresponding to the isolated A domain (Presland et al., 1997; Pearton et al., 2002). Interestingly, parallel analysis of epidermis from Matriptase/MT-SP1$^{-/-}$ littermates demonstrated the absence of both the proteolytically liberated S-100 protein and the isolated A domain. This was associated with the dramatic accumulation of a 50-kD protein previously identified as the intact S-100 protein linked to the first truncated filaggrin repeat (Fig. 5, lane 2; Pearton et al., 2002). This protein product was previously identified as a proteolytic processing intermediate that is rapidly converted into the mature S-100 protein in the normal epidermis, indicating that Matriptase/MT-SP1 is required for this specific processing step. An immu-

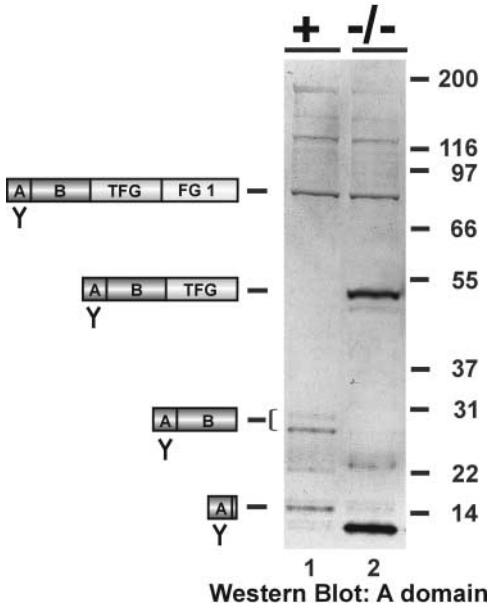

Figure 5. **Loss of proteolytic liberation of NH_2-terminal filaggrin S-100–containing protein products in Matriptase/MT-SP1–deficient epidermis.** Western blot analysis of epidermal protein extracts from control (lane 1) and littermate Matriptase/MT-SP1$^{-/-}$ (lane 2) neonates stained with the filaggrin S-100 A domain antibody. Control epidermis contains mature S-100 protein (28- and 30-kD doublets) and the isolated 16-kD S-100 A domain. In contrast, Matriptase/MT-SP1$^{-/-}$ epidermis contains no detectable S-100 protein, a dramatic accumulation of the 50-kD processing intermediate, and accumulation of an unidentified 10-kD filaggrin-related protein product. "A" and "B" indicate the A and B domains of the filaggrin S-100 protein, "TGF" indicates the truncated filaggrin repeat, and "FG 1" indicates the first filaggrin repeat.

noreactive 10-kD protein was also uniquely present in Matriptase/MT-SP1$^{-/-}$ epidermis, possibly representing the isolated EF hands of the A domain, formed as a consequence of impaired proteolytic liberation of the S-100 domain (Fig. 5, lane 2). The data show that loss of epidermal Matriptase/MT-SP1 impairs the proteolytic liberation of the NH_2-terminal filaggrin S-100 protein.

Prolonged exposure of Matriptase/MT-SP1–deficient skin to dehydration leads to severe ichthyosis

To determine if the epidermal barrier defect in Matriptase/MT-SP1$^{-/-}$ mice was caused by a transient and correctable delay in epidermal development or whether it could be rescued by systemic expression of Matriptase/MT-SP1, whole skin from Matriptase/MT-SP1$^{-/-}$ and littermate control neonates was transplanted to adult athymic nude mice. 3 wk after transplantation, the control grafts were covered with hair (Fig. 6 A, left), whereas skin from Matriptase/MT-SP1$^{-/-}$ mice presented with grotesque epidermal thickening and the formation of large plate-like epidermal scales (Fig. 6 A, right). Histologically, the grafted skin from control mice displayed a thin (2–3 cell layers) epidermis (Fig. 6 B) with low proliferation of basal keratinocytes (Fig. 6 D), characteristic of young adult skin. In stark contrast, transplanted Matriptase/MT-SP1$^{-/-}$ skin developed severe epidermal acanthosis (10–12 cell layers) and hyperkeratosis, with the formation of an extremely thick, compact stratum corneum (Fig. 6 C), pronounced hyperproliferation of basal keratinocytes as determined by BrdU incorporation (Fig. 6 E), and expression of the hyperproliferation-associated marker, keratin-6 (Fig. 6, compare F with G; Weiss et al., 1984). In contrast to control skin, erupted pelage hairs were almost absent in transplanted Matriptase/MT-SP1$^{-/-}$ skin (Fig. 6 A, right). Scanning EM examination of Matriptase/MT-SP1$^{-/-}$ skin occasionally revealed a few pelage hair shafts that uniformly presented as thin, broken fibers surrounded by dense sheaths of cornified debris (unpublished data). Matriptase/MT-SP1$^{-/-}$ epidermis displayed a profuse accumulation of aborted pelage hair follicle remnants embedded within the stratum corneum and a follicular infundibulum that was plugged by cornified material (unpublished data). Together, these data show that systemic expression of Matriptase/MT-SP1 does not correct the epidermal defects in Matriptase/MT-SP1$^{-/-}$ skin, and demonstrate a continuous requirement for keratinocyte Matriptase/MT-SP1 in epidermal differentiation.

Discussion

This paper demonstrates that the loss of keratinocyte Matriptase/MT-SP1 precipitates a plethora of defects in stratum corneum formation that compound to cause a cata-

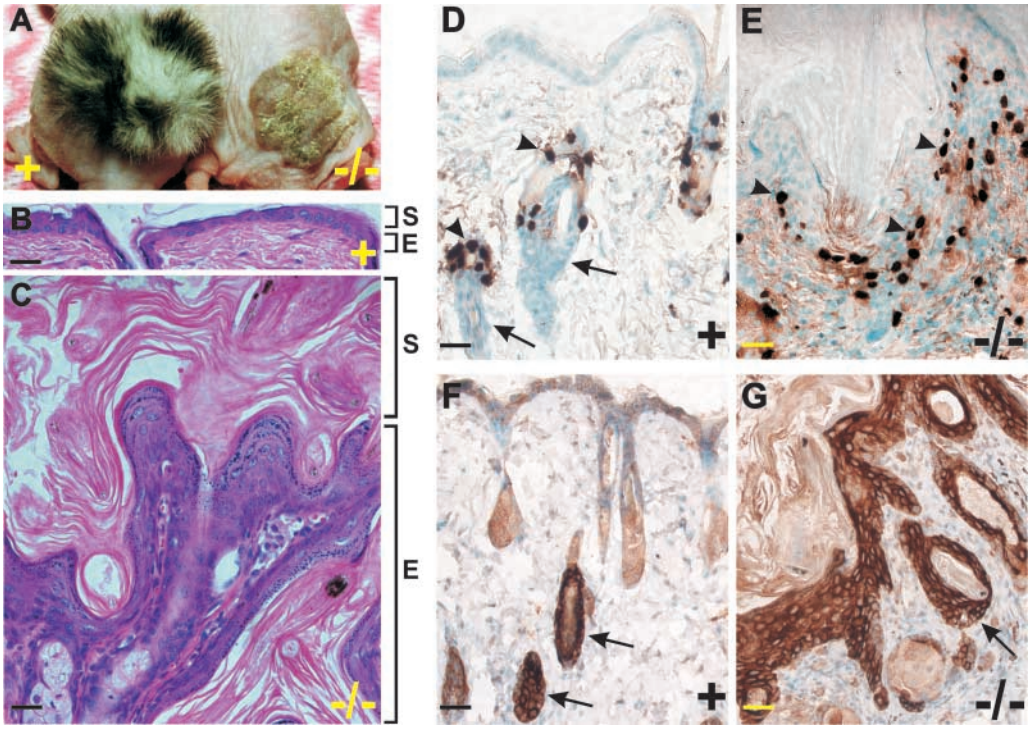

Figure 6. **Prolonged exposure of transplanted Matriptase/MT-SP1 epidermis to air leads to severe hyperproliferative ichthyosis.** Gross (A) and microscopic (B–G) appearance of control (B, D, and F) and Matriptase/MT-SP1$^{-/-}$ (C, E, and G) skin, 3 wk after transplantation to nude mice. Sections were stained with hematoxylin and eosin (B and C), or by immunostaining with anti-BrdU (D and E) or keratin-6 (F and G) antibodies. (A) Alopecia, grotesque epidermal thickening, and formation of epidermal plates in transplanted Matriptase/MT-SP1$^{-/-}$ skin. (B–G) Profound acanthosis and hyperkeratosis of transplanted Matriptase/MT-SP1$^{-/-}$ skin (compare B with C) with epidermal hyperproliferation (compare D with E) and keratin-6 overexpression (compare F with G). "E" in B and C indicates the location of basal and suprabasal epidermis, and "S" indicates the location of the stratum corneum. Examples of proliferating keratinocytes in the hair follicles (arrows) in D and in the epidermis in E are indicated with arrowheads. Keratin-6 staining of hair follicles (but not epidermis) in F, compared with strong keratin-6 staining of both epidermis and hair follicles in G. Bars, (B–G) 20 μm.

strophic loss of epidermal barrier function. The formation of the stratum corneum lipid matrix, CE morphogenesis, and desquamation were all shown to be Matriptase/MT-SP1–dependent. These defects correlated at the molecular level with the loss of the capacity to adequately proteolytically process epidermal profilaggrin, but not with detectable alterations in appearance of a range of other epidermal proteins, or with the proteolytic processing of epidermal transglutaminases. This specific proteolytic deficiency led to the selective loss of two prominent stratum corneum proteins, filaggrin monomer and filaggrin S-100 protein. The epidermal deficiency was not corrected with time or by systemic expression of Matriptase/MT-SP1, and prolonged exposure of barrier-deficient Matriptase/MT-SP1$^{-/-}$ skin to a dehydrating environment lead to the development of compensatory hyperproliferative ichthyosis.

Previous experiments have established clear links between defects in filaggrin and congenital ichthyosis, suggesting a direct causal relationship between Matriptase/MT-SP1 deficiency, loss of profilaggrin processing, and impaired barrier function. The flaky tail (ft) mouse mutant has lost the capacity to encode about half of the filaggrin monomer repeats, but not the S-100 protein (Presland et al., 2000). Newborn ft/ft mice present with an epidermal phenotype that is similar to (but somewhat milder than) Matriptase/MT-SP1 deficiency. The ft/ft phenotype includes dry, scaly skin with orthokeratotic hyperkeratosis. In humans, ichthyosis vulgaris is a heterogeneous and relatively common skin disorder with both autosomal dominant and recessive inheritance patterns (Francis, 1994; Compton et al., 2002). The clinical manifestations vary from mild to disfiguring scaling with painful fissuring, and at least some forms of the disease are associated with a reduction of profilaggrin expression, with the level of profilaggrin expression having been reported to correlate inversely with disease severity (Sybert et al., 1985). Harlequin ichthyosis is the most severe form of human congenital ichthyosis described thus far. Individuals affected by this rare autosomal recessive disorder usually die within the first few weeks of life and present with malformation of the stratum corneum, severely compromised epidermal barrier function, and large plate-like epidermal scales (Williams, 1992; Akiyama, 1999). Harlequin ichthyosis has been divided into three subtypes (I–III), based in part on the status of profilaggrin and filaggrin processing (Dale et al., 1990). Patients with type III disease lack detectable profilaggrin, whereas patients with type I and II disease have normal profilaggrin, but loss of proteolytic processing of profilaggrin. The epidermal defects in Harlequin ichthyosis patients also share several other features of Matriptase/MT-SP1–deficient mouse skin. These include hyperkeratosis, acanthosis, keratin-6 overexpression, lipid matrix defects, and impaired desquamation, but normal keratin-1, -5, -10, -14, loricrin, and transglutaminase expression (Hashimoto and Khan, 1992; Dale and Kam, 1993; Hashimoto et al., 1993; Nashi et al., 1993). In the light of these data, it is tempting to speculate that either the loss of filaggrin monomer and filaggrin S-100 protein from the upper epidermis or the incorporation of aberrantly processed profilaggrin into the stratum corneum may represent the central molecular event that precipitates the subsequent pleiotropic effects of Matriptase/MT-SP1 deficiency on epidermal development. Matriptase/MT-SP1 is the fourth protease to be implicated specifically in the complex series of proteolytic processing events that leads to the generation of filaggrin monomer and the filaggrin S-100 protein. Many molecular aspects of profilaggrin processing are still incompletely understood, due to the very peculiar properties of the profilaggrin protein (extreme insolubility and inability to be expressed as a recombinant protein) and the inability to mimic profilaggrin processing in cultured keratinocytes (see Introduction). This complex process includes multiple separate proteolytic cleavage events between the truncated filaggrin repeat and the first complete filaggrin repeat, between the S-100 protein and the first filaggrin repeat, the initial endoproteolytic cleavages of linker regions between filaggrin monomer repeats, and additional exo- or endoproteolytic trimming of the residual linker peptides. Terminal differentiation of keratinocytes is associated with dramatic changes in intracellular organelles and the plasma membrane that lead to cytoplasmic access of proteins normally located in the lumen of intracellular organelles or on the cell surface (Pearton et al., 2002). Pericellular, organelle-associated, and cytoplasmic proteases could therefore all potentially participate in the processing of profilaggrin. Matriptase/MT-SP1, although normally a cell surface–associated protease, could therefore have both direct functions in profilaggrin processing (profilaggrin cleavage and activation of profilaggrin-processing enzymes) and indirect functions (growth factor activation, ectodomain shedding, and ECM remodeling). With respect to the first possibility, it should be noted that the specific cleavage site between the truncated filaggrin repeat and the first filaggrin repeat in both mouse and human profilaggrin resembles the Matriptase/MT-SP1 consensus cleavage site defined previously (Takeuchi et al., 2000; Zhang et al., 2002), and that this cleavage of profilaggrin was clearly retarded in the Matriptase/MT-SP1$^{-/-}$ epidermis. The Matriptase/MT-SP1 consensus cleavage site is as follows: P4-(Arg/Lys)P3-(X)P2-(Ser)P1-(Arg)P1′-(Ala) or P4-(X)P3-(Arg/Lys)P2-(Ser)P1(Arg)P1′-(Ala). The mouse profilaggrin cleavage site is as follows: P4-(Arg)P3-(Arg)P2-(Ser)P1-(Arg)P1′-(Ala). The human profilaggrin cleavage site is as follows: (P4-(Arg)P3-(Lys)P2-(Arg)P1-(Arg)P1′-(Gly).

Matriptase/MT-SP1–deficient mice display hair follicle, hair canal, and thymic defects in addition to the loss of epidermal barrier function (List et al., 2002). It is noteworthy that profilaggrin is expressed in both follicular epidermis and thymic epithelium (Dale et al., 1985; Favre, 1989), and it is, therefore, quite possible that the loss of profilaggrin processing is the common molecular etiology of follicular, interfollicular, and thymic defects in Matriptase/MT-SP1$^{-/-}$ mice.

In conclusion, the data presented in these experiments have identified Matriptase/MT-SP1 as a novel and essential component of the profilaggrin-processing pathway and a key enzyme in terminal epidermal differentiation.

Materials and methods

Mice

Mice were generated and genotyped as described previously (Segre et al., 1999; List et al., 2002). The analysis of Matriptase/MT-SP1$^{-/-}$ mice was performed on two independent mouse strains, generated either as described previously (List et al., 2002) or by replacing exon 2 of Matriptase/MT-SP1 with a neomycin transferase expression cassette in E14.1 embryonic stem

cells. In all experiments, pairs of Matriptase/MT-SP1$^{-/-}$ and littermate control (Matriptase/MT-SP1$^{+/+}$ and $^{+/-}$) mice were used. Athymic nude-nu mice were purchased from Harlan. The experiment was performed in accordance with guidelines from the National Institutes of Health.

Histological and immunohistochemical analysis of epidermis

Histological and immunohistochemical analysis was performed as described previously (List et al., 2002). Tissue sections were stained with antibodies against keratin-1, -5, -6, -10, -14, and -16, loricrin, antibodies recognizing part of the filaggrin monomer repeat (DSQVHSGVQVEGRRGH; Covance), or the A domain of the NH_2-terminal S-100 protein (aa 38–52 in human profilaggrin; Zymed Laboratories). Cell proliferation was visualized by i.p. injection of 100 μg/g BrdU (Sigma-Aldrich) for 2 h before euthanasia and staining with anti-BrdU antibodies (DakoCytomation). Bound antibodies were visualized with a Vectastain® ABC peroxidase kit (Vector Laboratories) using DAB as the chromogenic substrate.

Immuno-EM

60-nm fixed tissue sections, generated as described previously (List et al., 2002), were placed on nickel grids, incubated in 50 mM glycine in PBS for 15 min, blocked in PBS with 5% BSA/5% goat serum and 0.1% cold water fish gelatin for 15 min, and in PBS with 0.1% Aurion BSA-C (Electron Microscopy Sciences) twice for 5 min. The sections were incubated with 10 μg/ml primary antibody in the above PBS/Aurion BSA-C for 1 h, washed six times for 5 min in PBS/Aurion BSA-C, and incubated in a 1:40 dilution of 6-nm gold–conjugated goat anti–rabbit IgG antibody (Electron Microscopy Sciences) in PBS/Aurion BSA-C for 1 h. Sections were washed six times for 5 min each with buffer, twice for 5 min each in PBS, fixed in 2% glutaraldehyde in PBS for 5 min, washed twice for 5 min in water, stained in uranyl acetate and lead citrate, and viewed under an electron microscope (model 100 CX-II; JEOL).

Ruthenium tetroxide transmission EM

The skin samples were processed essentially as described previously (Elias et al., 1998). In brief, 1-mm pieces were fixed overnight in 2.5% glutaraldehyde and 2% PFA in 0.1 M sodium cacodylate buffer, pH 7.4, at 4°C. The samples were post-fixed with 1% OsO_4 for 2 h in the dark and were incubated in 0.25% ruthenium tetroxide for 45 min, followed by dehydration and embedding. The blocks were polymerized at 68°C for 48 h. 80–90-nm "near-surface" sections were mounted on copper grids, stained with uranyl acetate and lead citrate, and examined with a transmission electron microscope (model 1010; JEOL) operated at 80 kV.

Tape stripping of epidermis

Neonates were killed by CO_2 inhalation, and the dorsal skin area was sequentially stripped with 14-mm D-Squame disks (Cuderm Corporation). The removed protein was quantitated as described previously (Dreher et al., 1998).

Preparation of CEs

CEs were purified and sonicated at 10 or 30°C for 30 min in a bath sonicator exactly as described previously (Koch et al., 2000).

Tissue protein extraction

Organs were homogenized on ice in 2% SDS, 10% glycerol, and 62.5 mM Tris-HCl, pH 6.8, sonicated three times for 15 s with a probe sonicator, and the lysate was cleared by centrifugation at 10,000 *g* for 10 min at 4°C. Neonatal epidermis was separated from dermis with forceps after heating the skin at 50°C for 3 min in PBS with 10 mM EDTA. Filaggrin and its precursors were purified from epidermis exactly as described previously (Resing et al., 1984).

Isolation of stratum corneum

The epidermis was suspended overnight at 4°C in 0.5% trypsin (TRL grade; Worthington Biochemical Company), rinsed in 20 mM PBS, pH 7.4, and 0.15 M NaCl overnight, rinsed in distilled water, retreated with fresh 0.5% trypsin in PBS for 2 h at RT, and rinsed in distilled water.

Epidermal lipid analysis

Lipids were extracted from desiccated epidermis and analyzed by TLC as described previously (Law et al., 1995).

cDNA array analysis

Array analysis was performed essentially as described previously (Teramoto et al., 2003). In brief, Cy-3– and Cy-5–labeled hybridization probes were generated from RNA isolated from neonate Matriptase/MT-SP1$^{-/-}$ and littermate control epidermis and used to screen mouse Mm-GEM2-v10p2_111602 cDNA arrays (NCI Microarray Facility, Gaithersburg, MD). Hybridized arrays were scanned (GenePix 4000A; Axon Instruments) and analyzed with GenePix Pro v3.0 (Axon Instruments) as described in the manufacturer's manual. The hybridization was repeated three times with independent sets of Matriptase/MT-SP1$^{-/-}$ and littermate control epidermis, reversing the fluorophores in one experiment. The complete list of the 8590 unique cDNAs included on the array is available upon request.

Protein identification by mass spectrometric peptide mapping

Proteins were separated by SDS-PAGE under reducing conditions. The gel was stained with amido black, and gel pieces in the region of interest were excised, rinsed, reduced, and alkylated before in-gel digestion with trypsin and analysis by MALDI mass spectrometry using a mass spectrometer (PerSeptive Voyager DE-RP; Applied Biosystems). Protein identification was performed by submitting the tryptic peptide masses for sequence database searches using MS-Fit/MS-Digest/ProteinProspector software (The Mass Spectrometry Facility of the University of California, San Francisco, CA) and the National Center for Biotechnology Information Entrez Protein database.

Western blot analysis

Western blot analysis was performed as described previously (Netzel-Arnett et al., 2002) using rabbit antibodies to mouse keratin-1, -5, -10, and -14, filaggrin, loricrin (Covance), claudin-1, profilaggrin (Zymed Laboratories), calpain-1 (Triple Point Biologics, Inc.), or protein phosphatase 2A (Upstate Biotechnology). Antibodies bound to the membrane were detected with alkaline phosphatase–conjugated porcine anti–rabbit or goat anti–mouse IgG (DakoCytomation).

RNA preparation and Northern blot analysis

RNA from neonatal skin was isolated and subjected to Northern blot analysis as described previously (List et al., 2002).

Skin grafting

Full-thickness dorsal skin grafts from neonate donor mice were transplanted onto athymic nude recipient mice as rectangular, 3–4-cm^2 split-thickness dorsal grafts. The grafts were secured with silk sutures, and Polysporin antibiotic ointment (Warner Lambert) was applied topically after surgery.

We thank Drs. J. Silvio Gutkind and Mary Jo Danton for critically reading the manuscript, Drs. William B. Swaim and Linda Bowers for EM, Dr. Mary Ann Gawinowicz for MALDI-MS, and Dr. Qian-Chun Yu for ruthenium EM. We also thank Dr. Pauline Wong for advice on skin transplantation, and David Mitola, Beth Burke, and Tricia Murdock for their excellent technical assistance.

K. List was supported by fellowships from Copenhagen University Hospital, the Danish Cancer Society, and the Svend Cole Frederiksen and Hustrus Foundation.

Submitted: 30 April 2003
Accepted: 2 October 2003

References

Akiyama, M. 1999. The pathogenesis of severe congenital ichthyosis of the neonate. *J. Dermatol. Sci.* 21:96–104.

Compton, J.G., J.J. DiGiovanna, K.A. Johnston, P. Fleckman, and S.J. Bale. 2002. Mapping of the associated phenotype of an absent granular layer in ichthyosis vulgaris to the epidermal differentiation complex on chromosome 1. *Exp. Dermatol.* 11:518–526.

Dale, B.A., K.A. Holbrook, and P.M. Steinert. 1978. Assembly of stratum corneum basic protein and keratin filaments in macrofibrils. *Nature.* 276:729–731.

Dale, B.A., K.A. Holbrook, J.R. Kimball, M. Hoff, and T.T. Sun. 1985. Expression of epidermal keratins and filaggrin during human fetal skin development. *J. Cell Biol.* 101:1257–1269.

Dale, B.A., K.A. Holbrook, P. Fleckman, J.R. Kimball, S. Brumbaugh, and V.P. Sybert. 1990. Heterogeneity in harlequin ichthyosis, an inborn error of epidermal keratinization: variable morphology and structural protein expression and a defect in lamellar granules. *J. Invest. Dermatol.* 94:6–18.

Dale, B.A., and E. Kam. 1993. Harlequin ichthyosis. Variability in expression and hypothesis for disease mechanism. *Arch. Dermatol.* 129:1471–1477.

Dreher, F., A. Arens, J.J. Hostynek, S. Mudumba, J. Ademola, and H.I. Maibach. 1998. Colorimetric method for quantifying human Stratum corneum removed by adhesive-tape stripping. *Acta Derm. Venereol.* 78:186–189.

Egelrud, T. 2000. Desquamation in the stratum corneum. *Acta Derm. Venereol. Suppl.* (*Stockh*). 208:44–45.

Elias, P.M., and G.K. Menon. 1991. Structural and lipid biochemical correlates of the epidermal permeability barrier. *Adv. Lipid Res.* 24:1–26.

Elias, P.M., C. Cullander, T. Mauro, U. Rassner, L. Komuves, B.E. Brown, and G.K. Menon. 1998. The secretory granular cell: the outermost granular cell as a specialized secretory cell. *J. Investig. Dermatol. Symp. Proc.* 3:87–100.

Favre, A. 1989. Identification of filaggrin in Hassall's corpuscle by histochemical and immunohistochemical methods. *Acta Anat.* (*Basel*). 135:71–76.

Francis, J.S. 1994. Genetic skin diseases. *Curr. Opin. Pediatr.* 6:447–453.

Hardman, M.J., P. Sisi, D.N. Banbury, and C. Byrne. 1998. Patterned acquisition of skin barrier function during development. *Development.* 125:1541–1552.

Hashimoto, K., and S. Khan. 1992. Harlequin fetus with abnormal lamellar granules and giant mitochondria. *J. Cutan. Pathol.* 19:247–252.

Hashimoto, K., G. De Dobbeleer, and T. Kanzaki. 1993. Electron microscopic studies of harlequin fetuses. *Pediatr. Dermatol.* 10:214–223.

Kim, M.G., C. Chen, M.S. Lyu, E.G. Cho, D. Park, C. Kozak, and R.H. Schwartz. 1999. Cloning and chromosomal mapping of a gene isolated from thymic stromal cells encoding a new mouse type II membrane serine protease, epithin, containing four LDL receptor modules and two CUB domains. *Immunogenetics.* 49:420–428.

Koch, P.J., P.A. de Viragh, E. Scharer, D. Bundman, M.A. Longley, J. Bickenbach, Y. Kawachi, Y. Suga, Z. Zhou, M. Huber, et al. 2000. Lessons from loricrin-deficient mice: compensatory mechanisms maintaining skin barrier function in the absence of a major cornified envelope protein. *J. Cell Biol.* 151:389–400.

Landmann, L. 1986. Epidermal permeability barrier: transformation of lamellar granule-disks into intercellular sheets by a membrane-fusion process, a freeze-fracture study. *J. Invest. Dermatol.* 87:202–209.

Law, S., P.W. Wertz, D.C. Swartzendruber, and C.A. Squier. 1995. Regional variation in content, composition and organization of porcine epithelial barrier lipids revealed by thin-layer chromatography and transmission electron microscopy. *Arch. Oral Biol.* 40:1085–1091.

Lin, C.Y., J. Anders, M. Johnson, and R.B. Dickson. 1999. Purification and characterization of a complex containing matriptase and a Kunitz-type serine protease inhibitor from human milk. *J. Biol. Chem.* 274:18237–18242.

List, K., C.C. Haudenschild, R. Szabo, W. Chen, S.M. Wahl, W. Swaim, L.H. Engelholm, N. Behrendt, and T.H. Bugge. 2002. Matriptase/MT-SP1 is required for postnatal survival, epidermal barrier function, hair follicle development, and thymic homeostasis. *Oncogene.* 21:3765–3779.

Marekov, L.N., and P.M. Steinert. 1998. Ceramides are bound to structural proteins of the human foreskin epidermal cornified cell envelope. *J. Biol. Chem.* 273:17763–17770.

Marttin, E., M.T. Neelissen-Subnel, F.H. De Haan, and H.E. Bodde. 1996. A critical comparison of methods to quantify stratum corneum removed by tape stripping. *Skin Pharmacol.* 9:69–77.

Nashi, H.K., A.V. Dhaded, and H.N. Nagarathna. 1993. Harlequin foetus. *Indian J. Pathol. Microbiol.* 36:483–485.

Nemes, Z., and P.M. Steinert. 1999. Bricks and mortar of the epidermal barrier. *Exp. Mol. Med.* 31:5–19.

Netzel-Arnett, S., D.J. Mitola, S.S. Yamada, K. Chrysovergis, K. Holmbeck, H. Birkedal-Hansen, and T.H. Bugge. 2002. Collagen dissolution by keratinocytes requires cell surface plasminogen activation and matrix metalloproteinase activity. *J. Biol. Chem.* 277:45154–45161.

Oberst, M., J. Anders, B. Xie, B. Singh, M. Ossandon, M. Johnson, R.B. Dickson, and C.Y. Lin. 2001. Matriptase and HAI-1 are expressed by normal and malignant epithelial cells in vitro and in vivo. *Am. J. Pathol.* 158:1301–1311.

Pearton, D.J., W. Nirunsuksiri, A. Rehemtulla, S.P. Lewis, R.B. Presland, and B.A. Dale. 2001. Proprotein convertase expression and localization in epidermis: evidence for multiple roles and substrates. *Exp. Dermatol.* 10:193–203.

Pearton, D.J., B.A. Dale, and R.B. Presland. 2002. Functional analysis of the profilaggrin N-terminal peptide: identification of domains that regulate nuclear and cytoplasmic distribution. *J. Invest. Dermatol.* 119:661–669.

Pierard, G.E., V. Goffin, T. Hermanns-Le, and C. Pierard-Franchimont. 2000. Corneocyte desquamation. *Int. J. Mol. Med.* 6:217–221.

Presland, R.B., P.V. Haydock, P. Fleckman, W. Nirunsuksiri, and B.A. Dale. 1992. Characterization of the human epidermal profilaggrin gene. Genomic organization and identification of an S-100-like calcium binding domain at the amino terminus. *J. Biol. Chem.* 267:23772–23781.

Presland, R.B., J.R. Kimball, M.B. Kautsky, S.P. Lewis, C.Y. Lo, and B.A. Dale. 1997. Evidence for specific proteolytic cleavage of the N-terminal domain of human profilaggrin during epidermal differentiation. *J. Invest. Dermatol.* 108:170–178.

Presland, R.B., and B.A. Dale. 2000. Epithelial structural proteins of the skin and oral cavity: function in health and disease. *Crit. Rev. Oral Biol. Med.* 11: 383–408.

Presland, R.B., D. Boggess, S.P. Lewis, C. Hull, P. Fleckman, and J.P. Sundberg. 2000. Loss of normal profilaggrin and filaggrin in flaky tail (ft/ft) mice: an animal model for the filaggrin-deficient skin disease ichthyosis vulgaris. *J. Invest. Dermatol.* 115:1072–1081.

Rawlings, A.V., I.R. Scott, C.R. Harding, and P.A. Bowser. 1994. Stratum corneum moisturization at the molecular level. *J. Invest. Dermatol.* 103:731–741.

Resing, K.A., K.A. Walsh, and B.A. Dale. 1984. Identification of two intermediates during processing of profilaggrin to filaggrin in neonatal mouse epidermis. *J. Cell Biol.* 99:1372–1378.

Resing, K.A., N. al-Alawi, C. Blomquist, P. Fleckman, and B.A. Dale. 1993. Independent regulation of two cytoplasmic processing stages of the intermediate filament-associated protein filaggrin and role of Ca^{2+} in the second stage. *J. Biol. Chem.* 268:25139–25145.

Resing, K.A., C. Thulin, K. Whiting, N. al-Alawi, and S. Mostad. 1995. Characterization of profilaggrin endoproteinase 1. A regulated cytoplasmic endoproteinase of epidermis. *J. Biol. Chem.* 270:28193–28198.

Roop, D. 1995. Defects in the barrier. *Science.* 267:474–475.

Rothnagel, J.A., and P.M. Steinert. 1990. The structure of the gene for mouse filaggrin and a comparison of the repeating units. *J. Biol. Chem.* 265:1862–1865.

Scott, I.R., and C.R. Harding. 1986. Filaggrin breakdown to water binding compounds during development of the rat stratum corneum is controlled by the water activity of the environment. *Dev. Biol.* 115:84–92.

Segre, J.A., C. Bauer, and E. Fuchs. 1999. Klf4 is a transcription factor required for establishing the barrier function of the skin. *Nat. Genet.* 22:356–360.

Simon, M., M. Haftek, M. Sebbag, M. Montezin, E. Girbal-Neuhauser, D. Schmitt, and G. Serre. 1996. Evidence that filaggrin is a component of cornified cell envelopes in human plantar epidermis. *Biochem. J.* 317:173–177.

Steinert, P.M., and L.N. Marekov. 1995. The proteins elafin, filaggrin, keratin intermediate filaments, loricrin, and small proline-rich proteins 1 and 2 are isodipeptide cross-linked components of the human epidermal cornified cell envelope. *J. Biol. Chem.* 270:17702–17711.

Steven, A.C., and P.M. Steinert. 1994. Protein composition of cornified cell envelopes of epidermal keratinocytes. *J. Cell Sci.* 107:693–700.

Swartzendruber, D.C., P.W. Wertz, K.C. Madison, and D.T. Downing. 1987. Evidence that the corneocyte has a chemically bound lipid envelope. *J. Invest. Dermatol.* 88:709–713.

Sybert, V.P., B.A. Dale, and K.A. Holbrook. 1985. Ichthyosis vulgaris: identification of a defect in synthesis of filaggrin correlated with an absence of keratohyaline granules. *J. Invest. Dermatol.* 84:191–194.

Takeuchi, T., M.A. Shuman, and C.S. Craik. 1999. Reverse biochemistry: use of macromolecular protease inhibitors to dissect complex biological processes and identify a membrane-type serine protease in epithelial cancer and normal tissue. *Proc. Natl. Acad. Sci. USA.* 96:11054–11061.

Takeuchi, T., J.L. Harris, W. Huang, K.W. Yan, S.R. Coughlin, and C.S. Craik. 2000. Cellular localization of membrane-type serine protease 1 and identification of protease-activated receptor-2 and single-chain urokinase-type plasminogen activator as substrates. *J. Biol. Chem.* 275:26333–26342.

Teramoto, H., R.L. Malek, B. Behbahani, M.D. Castellone, N.H. Lee, and J.S. Gutkind. 2003. Identification of H-Ras, RhoA, Rac1 and Cdc42 responsive genes. *Oncogene.* 22:2689–2697.

Weiss, R.A., R. Eichner, and T.T. Sun. 1984. Monoclonal antibody analysis of keratin expression in epidermal diseases: a 48- and 56-kdalton keratin as molecular markers for hyperproliferative keratinocytes. *J. Cell Biol.* 98:1397–1406.

Wertz, P.W. 2000. Lipids and barrier function of the skin. *Acta Derm. Venereol. Suppl.* (*Stockh*). 208:7–11.

Wertz, P.W., and B. van den Bergh. 1998. The physical, chemical and functional properties of lipids in the skin and other biological barriers. *Chem Physiol. Lipids.* 91:85–96.

Wertz, P.W., K.C. Madison, and D.T. Downing. 1989. Covalently bound lipids of human stratum corneum. *J. Invest. Dermatol.* 92:109–111.

Williams, M.L. 1992. Ichthyosis: mechanisms of disease. *Pediatr. Dermatol.* 9:365–368.

Zhang, D., S. Karunaratne, M. Kessler, D. Mahony, and J.A. Rothnagel. 2002. Characterization of mouse profilaggrin: evidence for nuclear engulfment and translocation of the profilaggrin B-domain during epidermal differentiation. *J. Invest. Dermatol.* 119:905–912.